**Title**
RESERVOIR ENGINEERING OF SHALLOW, FAULT-CHARGED HYDROTHERMAL SYSTEMS



**Authors**
Benson, S.M.
Bodvarsson, G.S.
Mangold, D.C.

**Publication Date**
1981-12-01

# Lawrence Berkeley Laboratory

UNIVERSITY OF CALIFORNIA



## EARTH SCIENCES DIVISION

Presented at the Stanford Seventh Annual Geothermal Workshop, University of California, Stanford, CA, December 15-17, 1981

RESERVOIR ENGINEERING OF SHALLOW, FAULT-CHARGED HYDROTHERMAL SYSTEMS

S.M. Benson, G.S. Bodvarsson, and D.C. Mangold

December 1981



Prepared for the U.S. Department of Energy under Contract DE-AC03-76SF00098

## DISCLAIMER

LBL-13271

# RESERVOIR ENGINEERING OF SHALLOW, FAULT-CHARGED HYDROTHERMAL SYSTEMS

S.M. Benson, G.S. Bodvarsson, and D.C. Mangold

Earth Sciences Division
Lawrence Berkeley Laboratory
University of California
Berkeley, California 94720

December 1981

This work was supported by the Assistant Secretary for Conservation and Renewable Energy, Office of Renewable Technology, Division of Geothermal and Hydropower Technologies of the U.S. Department of Energy under Contract No. DE-AC03-76SF00098.

## INTRODUCTION

Many of the low- to moderate-temperature (<150°C) geothermal resources being developed in the United States are in near-surface aquifers. These shallow thermal anomalies, typical of the Basin and Range and Cascades Provinces, are attributed to hydrothermal circulation. The aquifers are commonly associated with faults, fractures, and complex geological settings; they are usually very limited in size and display temperature inversions with depth. Because of the shallow depths and warm temperatures of these resources, they are attractive for development of direct-use hydrothermal energy projects. However, development of the resources is hindered by their complexity, the typically limited manifestation of the resources, and the lack of established reservoir engineering and assessment methodology.

In this paper a conceptual model of these systems is postulated, a semianalytic computational model is developed, and reservoir engineering methods (including calculation of reservoir longevity, pressure-transient analysis, and well-siting strategy) are re-evaluated to include the reservoir dynamics necessary to explain such systems. Finally, the techniques are applied to the Susanville, California, hydrothermal anomaly.

## THERMAL MODEL

Figure 1 shows a schematic of the conceptual model developed to explain the occurrence of near-surface hot water aquifers. Hot water rises along a fault until a highly permeable aquifer is intersected. As the hot water moves away from the fault, it is cooled by equilibration with aquifer rock and by heat conduction to the overlying and underlying rock units. The model discussed in this paper is most applicable to thin aquifers, as vertical temperature variations in the aquifer are not considered.

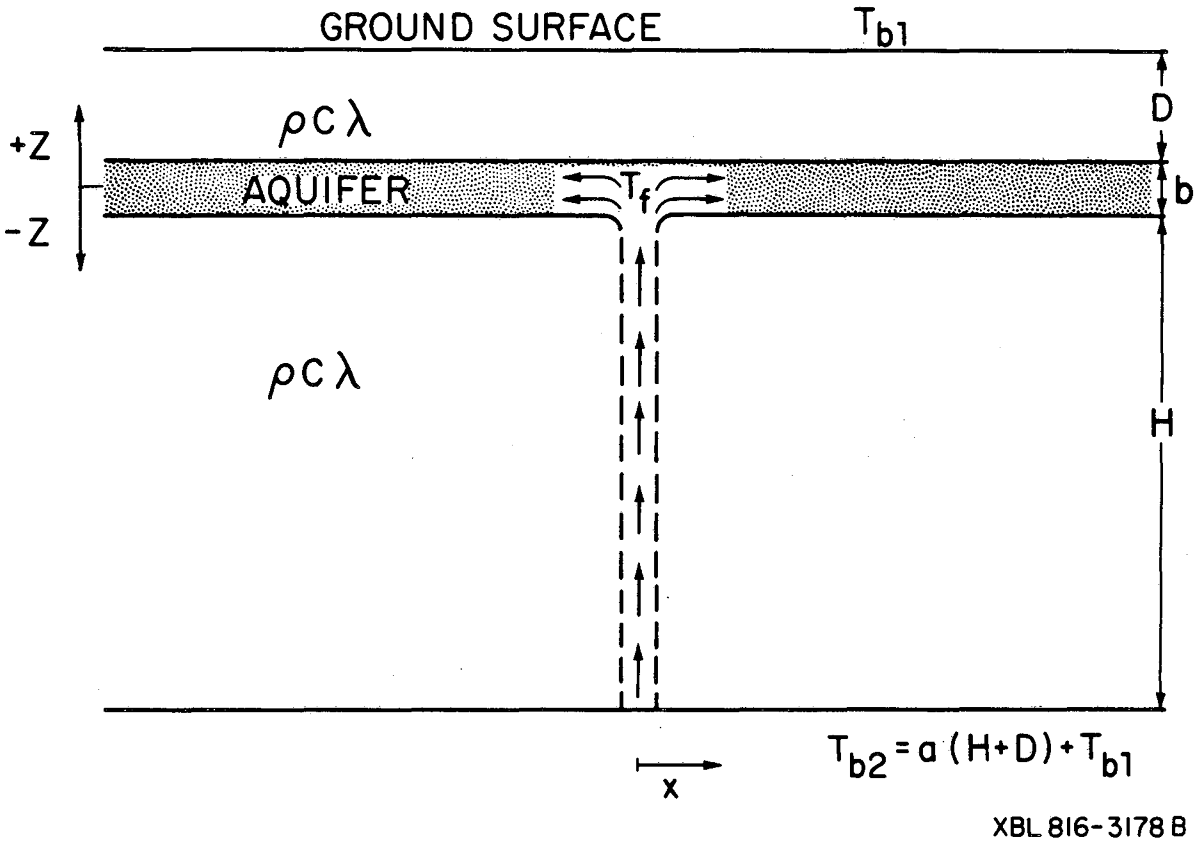


Figure 1. Schematic of a conceptual model for a fault-charged hydrothermal system.

A semianalytic model has been developed to calculate the temperature distribution of the system as a function of the flow rate into the aquifer, the temperature of the water entering the aquifer, initial linear temperature profile, system geometry, rock properties, and time (Bodvarsson et al., 1981). The primary assumptions are listed below:

1. In the aquifer, the mass flow is steady, horizontal conduction is neglected, and temperature is uniform in the vertical direction (thin aquifer). Thermal equilibrium between the fluid and the solids is instantaneous.

2. The rock matrix above and below the aquifer is impermeable. Horizontal conduction in the rock matrix is neglected.

3. The energy resistance at the contact between the aquifer and the rock matrix is negligible (instantaneous rock-fluid equilibration).

4. The thermal properties of the formations above and below the aquifer are the same, and the thermal parameters of the liquid and the rocks are constant.

The differential equation governing the temperature in the aquifer at any time (t) can be readily derived by performing an energy balance on a control volume in the aquifer:

$$z = 0: \quad \frac{\lambda}{b} \left. \frac{\partial T_1}{\partial z} \right|_{z=0} - \frac{\lambda}{b} \left. \frac{\partial T_2}{\partial z} \right|_{z=0} - \frac{\rho_w c_w q}{b} \frac{\partial T_a}{\partial x} - \rho_a c_a \frac{\partial T_a}{\partial t} = 0 \ . \tag{1}$$

The symbols are defined in the nomenclature. In the caprock and the bedrock, the one-dimensional heat-conduction equation controls the temperature:

$$z > 0: \quad \lambda \frac{\partial^2 T_1}{\partial z^2} = \rho_r c_r \frac{\partial T_1}{\partial t}, \tag{2}$$

$$z < 0: \quad \lambda \frac{\partial^2 T_2}{\partial z^2} = \rho_r c_r \frac{\partial T_2}{\partial t}. \tag{3}$$

The initial conditions are:

$$\begin{aligned} T_a(x,0) &= T_1(x,z,0) = T_2(x,z,0) \\ &= T_{b1} - a(z - D). \end{aligned} \tag{4}$$

The boundary conditions are:

$$T_a(0,t) = T_f, \; t > 0, \tag{5a}$$

$$T_a(x,t) = T_1(x,0,t) = T_2(x,0,t), \tag{5b}$$

$$T_1(x,D,t) = T_{b1}, \tag{5c}$$

$$T_2(x,-H,t) = T_{b2} = T_{b1} + a(H + D). \tag{5d}$$

The following dimensionless parameters are introduced:

$$\xi = \frac{\lambda x}{\rho_w c_w q D}, \qquad \tau = \frac{\lambda t}{\rho_r c_r D^2}; \tag{6a,b}$$

$$\theta = \frac{b}{D} \frac{\rho_a c_a}{\rho_r c_r} , \qquad \eta = \frac{z}{D} ; \tag{6c,d}$$

$$T_D = \frac{T - T_{b1}}{T_f - T_{b1}} , \qquad T_g = \frac{aD}{T_f - T_{b1}} ; \tag{6e,f}$$

$$\alpha = H/D . \tag{6g}$$

The solution of equations (1) to (3) can be easily obtained in the Laplace domain (Bodvarsson, 1981).

$$\eta = 0: \quad \mu = \frac{1}{p} [1 - T_g] \cdot \exp - \left[ \theta p + \frac{\sqrt{p}}{\tanh \sqrt{p}} + \frac{\sqrt{p}}{\tanh \sqrt{p\alpha}} + \frac{T_g}{p} \right] . \tag{7}$$

$$\eta > 0: \quad v = \left[ u - (T_g/p) \right] \cosh \eta\sqrt{p} - \frac{\left[ u - (T_g/p) \right]}{\tanh \sqrt{p}} \sinh \eta\sqrt{p} - \frac{T_g}{p} (\eta - 1) . \tag{8}$$

$$\eta < 0: \quad w = \left[ u - (T_g/p) \right] \cosh \eta\sqrt{p} + \frac{\left[ u_g - (T_g/p) \right]}{\tanh (\alpha\sqrt{p}} \sinh \eta\sqrt{p} - \frac{T_g}{p} (\eta - 1) . \tag{9}$$

In equations (7) to (9), u, v, and w represent the temperature in the Laplace domain of the aquifer, the rock above the aquifer, and the rock below the aquifer, respectively. As equations (7) to (9) cannot easily be inverted from the Laplace domain, a numerical inverter was used to evaluate the equations.

This model can be used to study the evolution of these systems. Figure 2 shows the evolution of a hypothetical system. The dimensionless coordinates used are defined in equations (6a) to (6g). In simple terms, the graph can be envisioned as the evolution of a single temperature profile at a given location ($\xi$) away from the fault. Before the incidence of hydrothermal circulation, the temperature profile is linear (normal geothermal gradient). When water begins to flow up the fault and into the aquifer, the aquifer begins to heat up. The fluid flows laterally in the aquifer, losing heat by conduction to the cap rock and basement. A distinctive temperature reversal forms below the aquifer. With increasing time, conductive heat losses to the cap rock stabilize and a typical linear conductive gradient is established above the aquifer. At very large times, the temperature below the aquifer stabilizes and, for the case considered, becomes nearly constant with depth.

Another application of this model is to calculate the rate of hot water recharge into an aquifer, given sufficient information about the areal and vertical temperature distribution in the aquifer. The model has been applied to the Susanville, California, hydrothermal resource, a low-temperature system located at the intersection of the Basin and Range Province, the Sierra Nevada, and the Modoc Plateau. Data from more than twenty shallow exploration and production wells have outlined a thermal anomaly which is elongated around a northwest-trending axis (Benson et al., 1980). Temperature

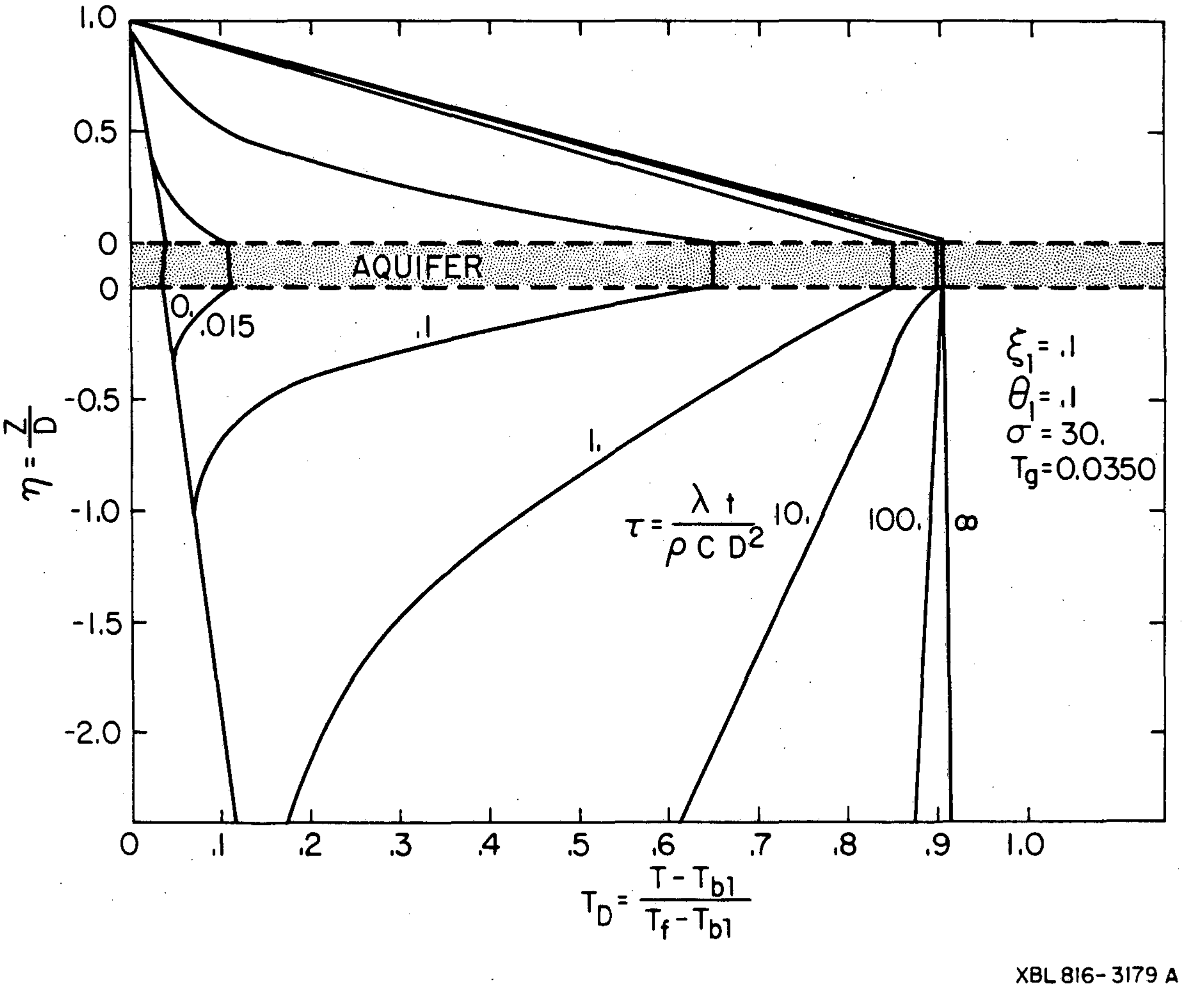


Figure 2. Evolution of a fault-charged hydrothermal system. This schematic represents the evolution of a single temperature profile over time. The dimensionless coordinates used are defined in equations (6a) through (6g).

contours at a depth of approximately 125 m below the surface (elevation 1150 m) are shown in Figure 3. Temperature profiles from several of the wells are shown in Figure 4. In each well, temperatures increase linearly with depth to about 125 m below the surface. At greater depths, the temperatures remain isothermal or have a reversal. The shape of the thermal anomaly can be explained as due to a recharging fault, which is slightly to the east of well Suzy 9 and aligned with the northwest trend of the anomaly. The match of calculated and observed temperatures shown in Figure 4 was obtained by assuming a hot water recharge rate (80°C) of $9 \times 10^{-6}$ $m^3/s/m$ (obtained by trial and error) along the length of the fault. The remaining parameters used to obtain this match are shown in Table 1. Temperature contours were

Table 1. Parameters used for the Susanville model.

| Parameter | Units |
|---|---|
| Geothermal gradient, a | 3°C/100 m |
| Aquifer thickness, b | 35 m |
| Depth to aquifer, D | 125 m |
| Aquifer porosity, $\phi$ | 0.2 |
| Thermal conductivity of rock, $\lambda$ | 1.5 J/m·s·°C |
| Rock heat capacity, c | 1000 J/kg·°C |
| Rock density, $\rho$ | 2700 $kg/m^3$ |
| Ground level temperature, Tb1 | 10°C |
| Lower temperature limit (case 1), Tb2 | 130°C at 4 km |
| Lower temperature limit (case 2), Tb2 | 22°C at 400 m |

also considered for the match of the calculated and observed temperature distribution. A match using the same recharge rate ($9 \times 10^{-6}$ $m^3/s/m$) and recharge temperature (80°C) is shown in Figure 5. The match of observed and calculated values is very good close to the recharging fault. However,

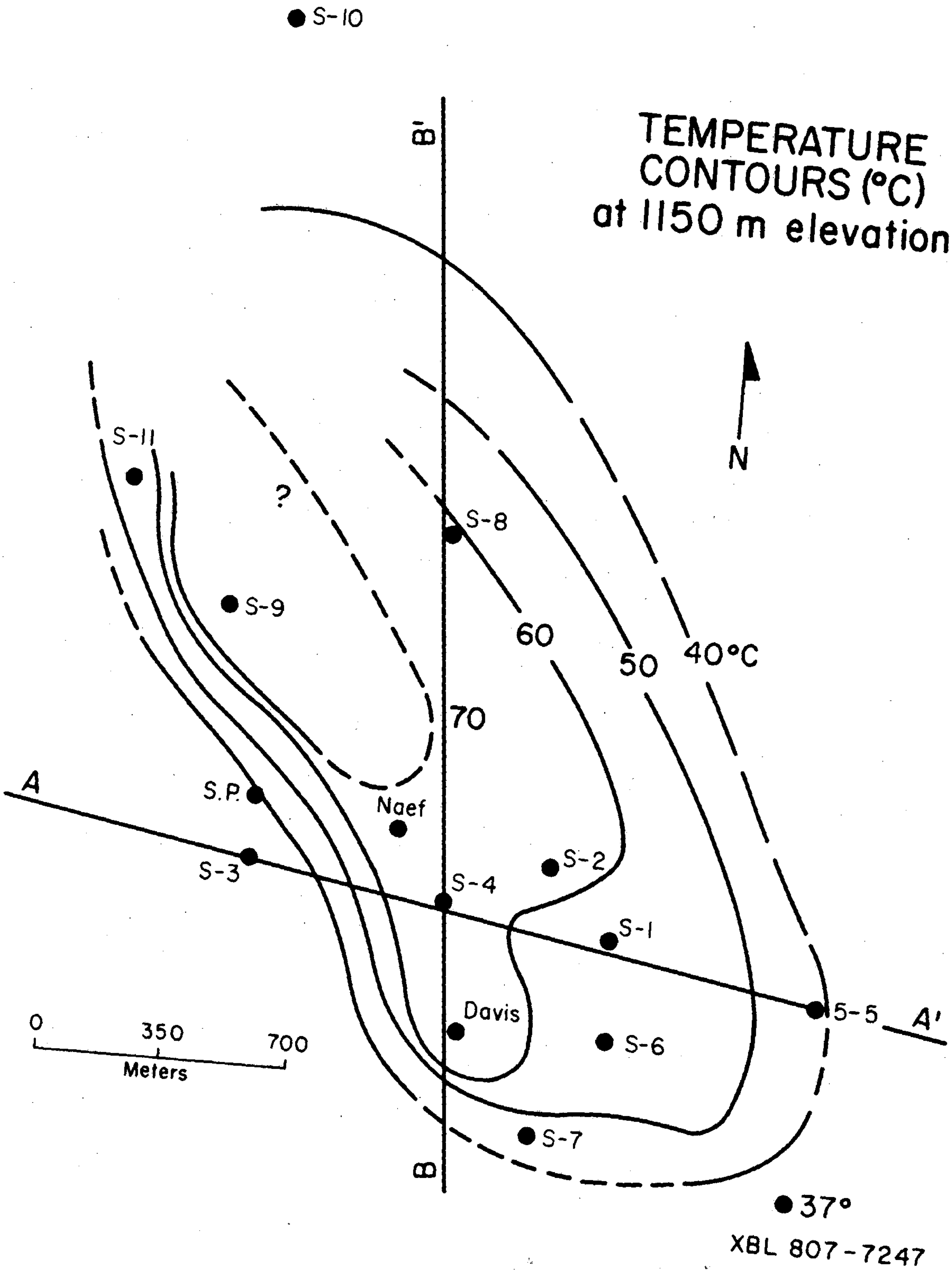


Figure 3. Temperature contours at 125 m depth (1150 m elevation) at Susanville, California.

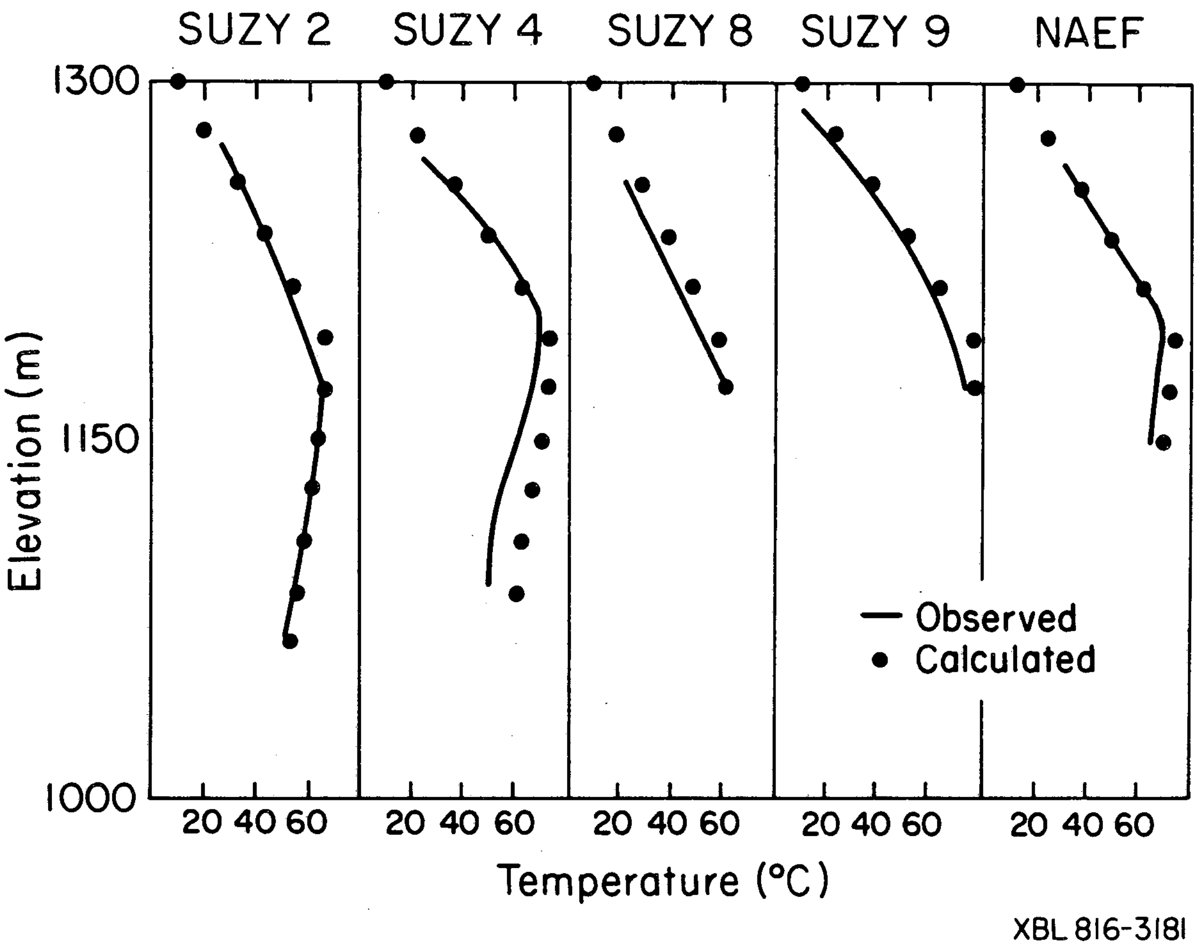


Figure 4. Temperature profiles for several of the Susanville wells, demonstrating temperature reversals with depth. Also plotted are the temperature profiles calculated using the semianalytic model.

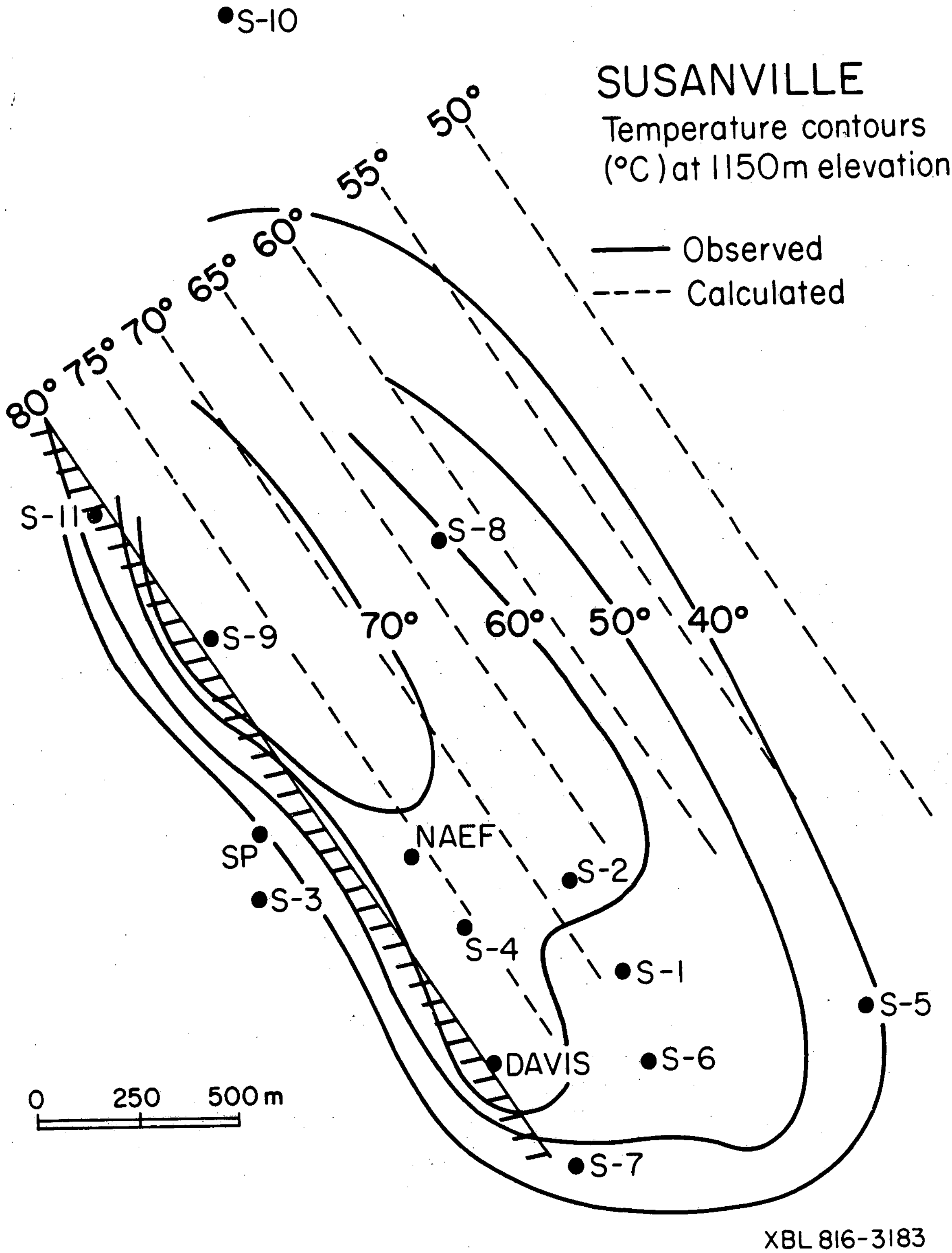


Figure 5. Match of calculated and observed temperature contours at Susanville.

farther from the fault the match is not very good. The discrepancy could be due to any number of factors: the regional flow of cold water from the northwest, the complexity of the geologic setting, the downflow of hot fluids at a distance from the fault, or the inaccuracy inherent in modeling a three-dimensional phenomenon in two dimensions.

The match shown in Figures 4 and 5 was obtained using two different sets of boundary conditions: (1) if the lower constant-temperature boundary is placed very deep (H >> D), the parameters obtained indicate that the hydrothermal system has been evolving for approximately 2000 years and that the fault charges the system at a rate of $9 \times 10^{-6}$ $m^3/s/m$; (2) placing a constant-temperature boundary (22°C) at a depth of about 400 m results in a very similar match. In the second case, steady-state temperature conditions are reached (consequently, the evolution time can be determined only as exceeding 10,000 years), but the calculated recharge rate is the same as in the first case ($9 \times 10^{-6}$ $m^3/s/m$). If one considers the age of the subsurface formations at Susanville, the second case seems more likely.

## HYDROTHERMAL SIMULATION

In order to predict the useful lifetime of a fault-charged system, it is necessary to determine the effects of the hot water recharge on longevity, pressure-transient behavior, and well-siting strategy. A simple criterion for reservoir longevity was used: maintenance of sufficiently high production temperature. Because these systems are often highly nonisothermal and because transient thermal phenomena are important, a numerical simulator must be used to model the response of a fault-charged reservoir to pressure-transient testing and sustained production from a well.

The recently developed numerical simulator PT (pressure-temperature) was used. This simulator solves the mass and energy transport equations for liquid-saturated heterogeneous porous and/or fractured media. It includes the temperature dependence of fluid density, viscosity, and expansivity in the calculations, and uses the integrated finite-difference method to discretize the medium and formulate the governing equations. The set of linear equations arising at each timestep is solved by direct means, using an efficient sparse solver. A detailed description of the simulator is given by Bodvarsson (1982).

To demonstrate the application of a numerical simulator to a fault-charged reservoir, the Susanville hydrothermal system was modeled. The geometry of the system was determined by correlation of well logs, drill cuttings, and temperature profiles. Although the system is highly complex, a simplified model of the system which accounts for the major hydrothermal features was used. A cross section of the aquifer model and confining strata is shown in Figure 6. A 35-m-thick aquifer with a permeability of 2 darcies is overlain by an impermeable cap rock and underlain by 240 m of impermeable bedrock. The ground surface temperature is a constant 10°C. The temperature at the bottom of the section (400 m depth) is a constant 22°C. To determine the temperature everywhere else in the system, the analytic solution discussed in the previous section was used, incorporating a recharge rate of $9 \times 10^{-6}$ $m^3/s/m$ (at 80°C). This temperature distribution is close to the measured temperature distribution (see above).

The initial temperature and pressure distributions in the aquifer as a function of distance from the fault are shown in Figure 7. The pressure distribution in the aquifer was calculated so that the fault would sustain a

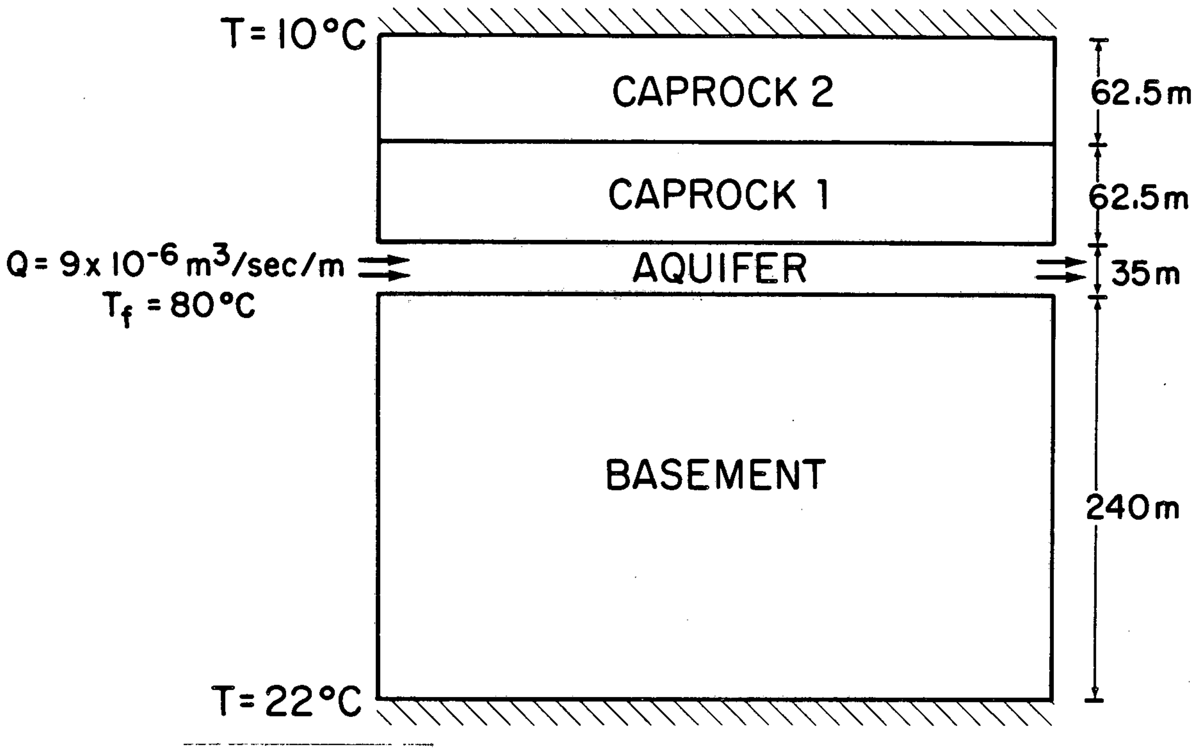


Figure 6. Cross section of the reservoir model used for numerical simulation of the Susanville hydrothermal system, showing the four layers used in the mesh, the boundary conditions, and the aquifer location.

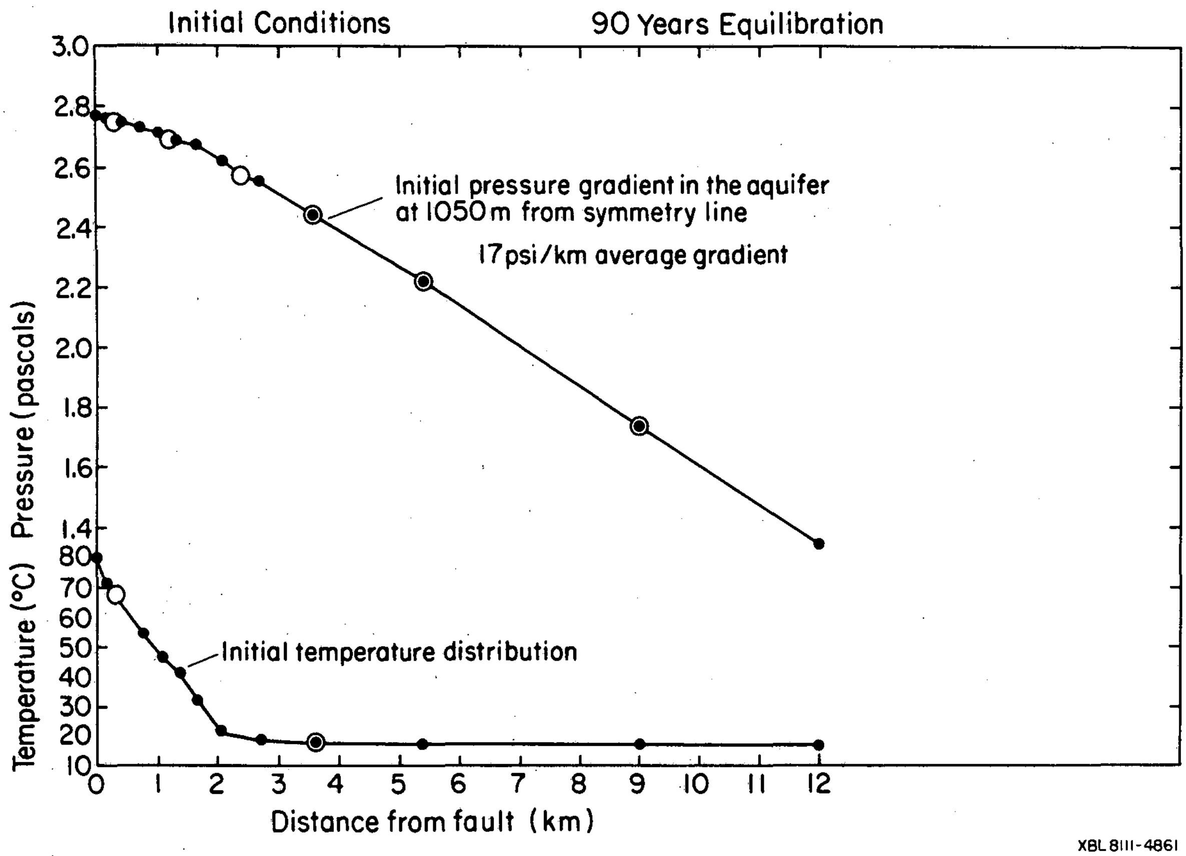


Figure 7. Initial pressure and temperature distribution in the aquifer.

rate of 9 x $10^{-6}$ $m^3/s/m$. As shown in Figure 7, the pressure gradient close to the fault is smaller than that far from the fault, where it is approximately 17 psi/km. This is as expected, because the fluid viscosity close to the fault is less than half the viscosity of the 20°C fluid far from the fault. A constant-potential boundary condition was imposed at the downstream end of the aquifer. At the fault, two different boundary conditions were imposed: constant potential and constant flow. A four-layer mesh (see Figure 6) was used to model this problem. The same mesh was used for each layer; a plane view of one such layer is shown in Figure 8. Only half of the flow field is modeled because of the symmetry of the problem.

RESERVOIR LONGEVITY

The first objective of this simulation was to determine the production temperature vs. time for a well located 600 m from the fault. The initial temperature at the production well was 59°C. The well was then produced at a rate of 31 kg/s (500 gpm). Figure 9 shows a plot of the production temperature over a 30-year lifetime for two cases: one with a constant-potential fault and one in which the fault maintains a constant flow. In the case of constant flow rate, the temperature remained nearly constant during the 30-year lifetime; only near the end of the period did the temperature begin to decline. In the case of constant potential, the temperature gradually increased with time; during the 30-year period the production temperature increased from 60°C to 67°C. This increase in temperature is readily explained by the increased rate of flow from the fault, which results from the production-induced drawdown near the fault. Figure 10 shows a plot of recharge rate vs. distance from the line of symmetry. Near the production well, the recharge rate was nearly three times as great as the steady value which created the

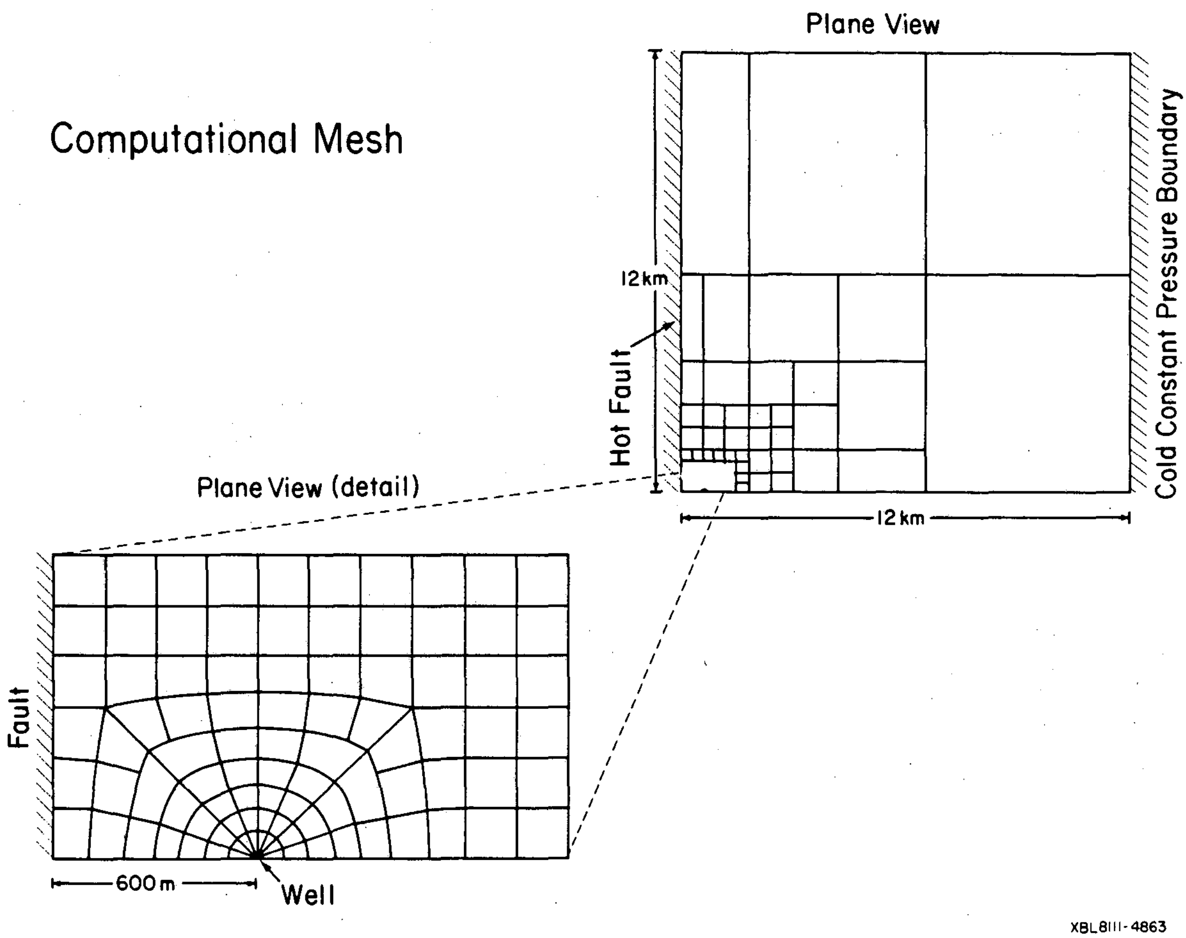


Figure 8. Plane view of the mesh used for the numerical simulations.

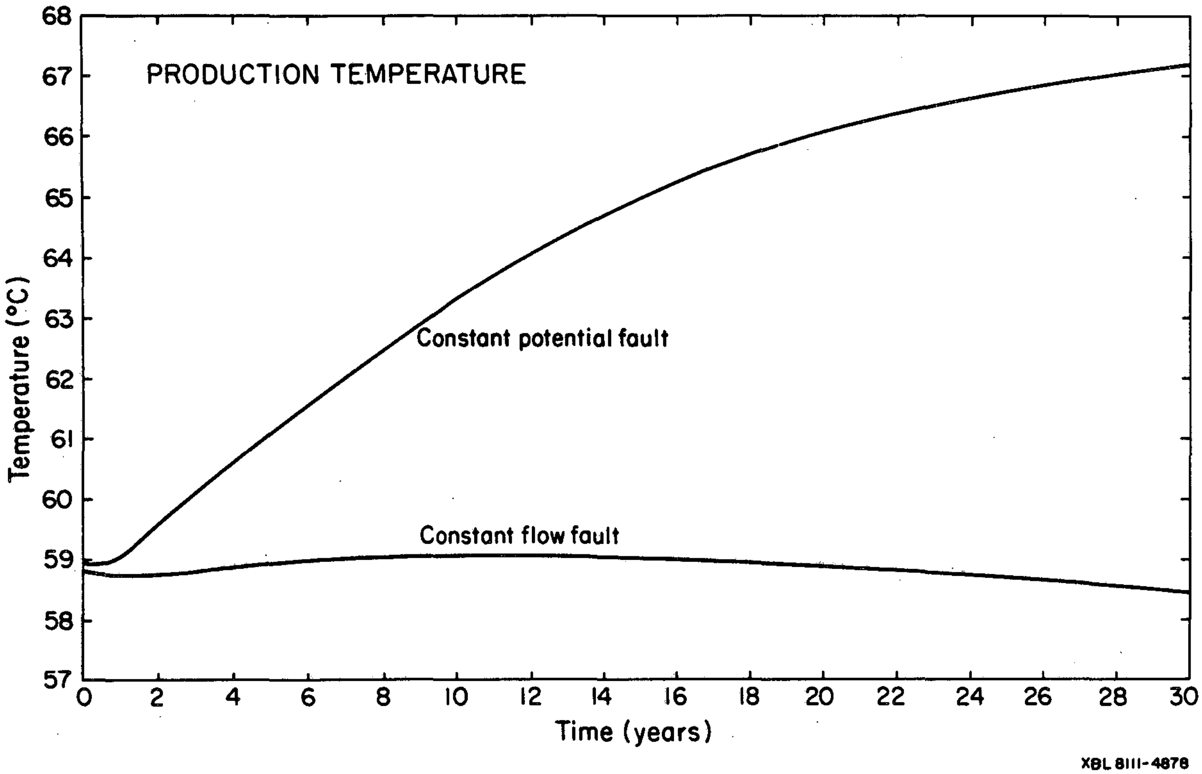


Figure 9. Production temperature vs. time for a well producing from a fault-charged reservoir for two cases: (1) a constant-potential fault and (2) a constant-flow fault.

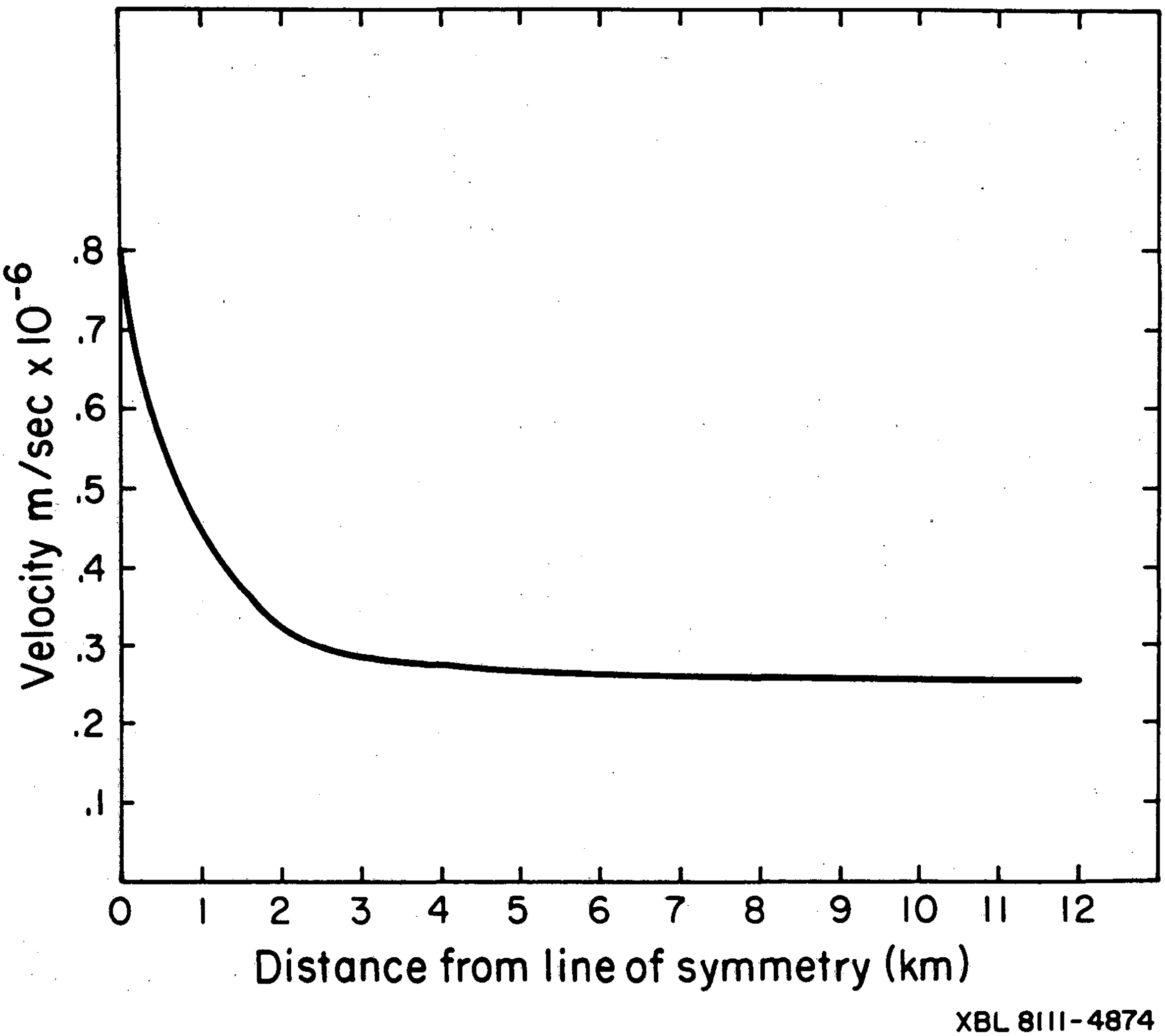


Figure 10. Flow rate from a constant-potential fault near a well being produced at 31 kg/s (after 30 years of production).

initial thermal anomaly. Figure 11 compares initial temperature contours with those after 30 years of production. As illustrated, the more mobile hot water moved quickly toward the production well, causing the production temperature to increase. The cold water also moved toward the production well, but at a slower rate.

This simulation demonstrates that for fault-charged hydrothermal systems, it is critical to include the recharge in order to obtain an accurate reservoir assessment. If no recharge is considered, then all of the hot water initially within the 60°C contour will be removed within 10 years [at a rate of 31 kg/s (500 gpm)]. Both of the other cases (constant potential and constant flow) demonstrate that the resource will be adequate for a miniumum of 30 years. The constant-potential case suggests that the resource may be enhanced by exploitation. The nature of the recharging fault is clearly a key to understanding and effectively exploiting these systems.

PRESSURE TRANSIENT ANALYSIS

The same mesh and reservoir parameters were used to simulate a 30-day production/interference test in a fault-charged reservoir. The production well was produced at a constant rate of 31 kg/s, and pressure changes were observed in the production well and two interference wells. Figure 12 shows a semilog plot of the pressure-transient data from the production well. As expected, the early-time data form a straight line and later stabilize, indicating a constant-potential boundary. Analysis of the production well data gave a transmissivity of $4.8 \times 10^5$ md·ft/cp, the value used in the simulation (corresponding to the fluid viscosity at 60°C).

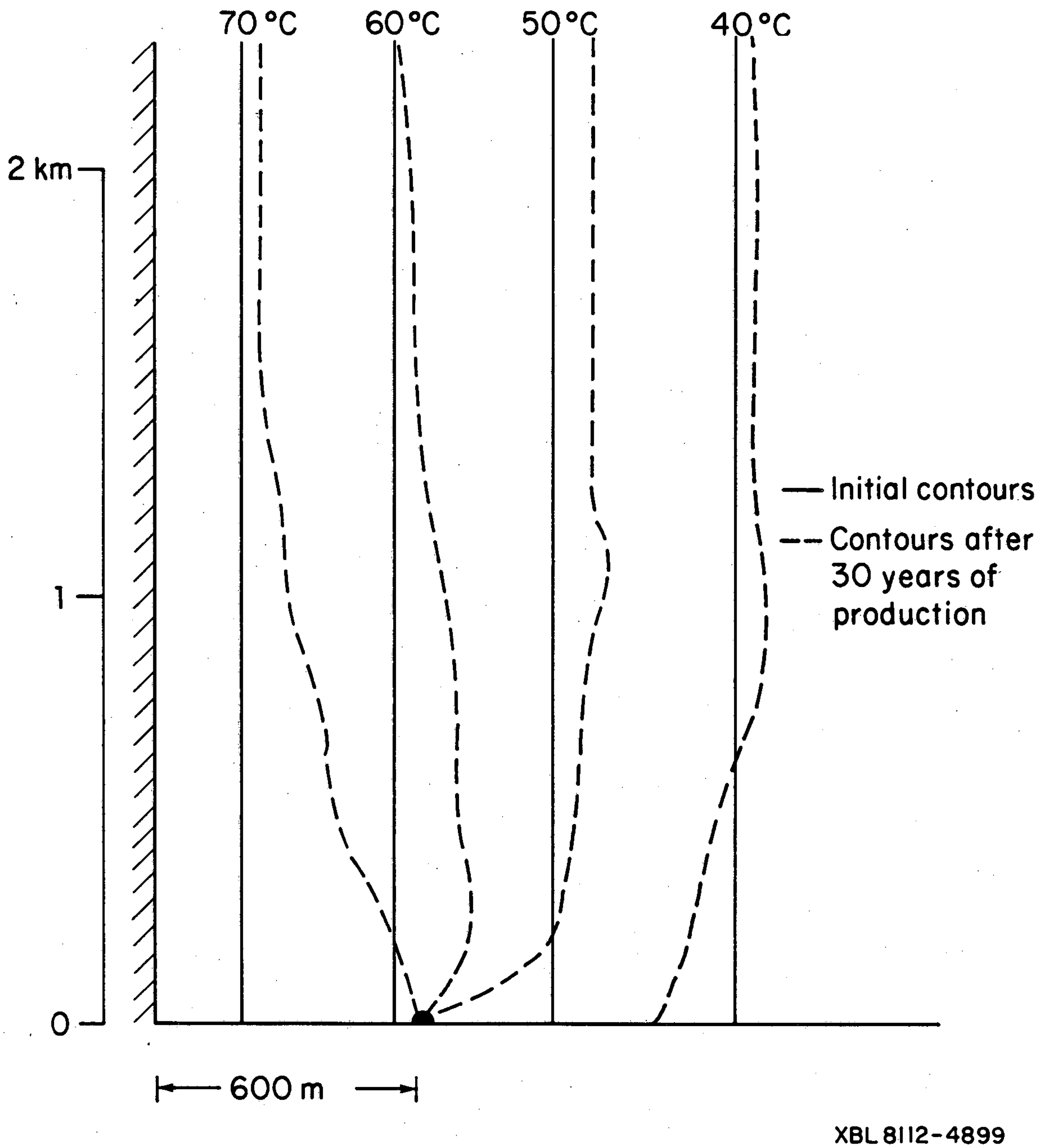


Figure 11. Comparison of temperature contours between their initial value and after 30 years of production from a well in a reservoir bounded by a constant-potential fault.

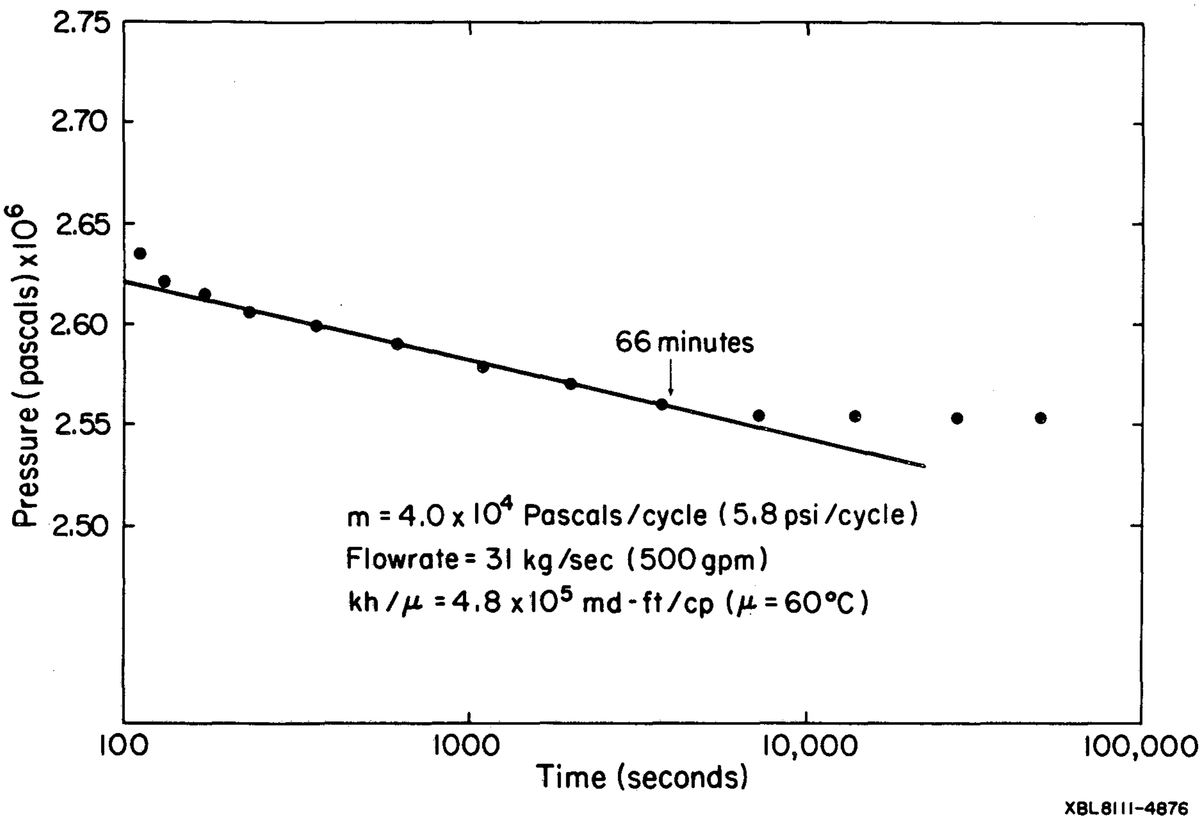


Figure 12. Drawdown and semilog analysis of data from a production well in a reservoir bounded by a constant-potential fault.

The inset in Figure 13 is a schematic of the well locations and the drawdowns at the observation wells for the constant-potential fault case. At early times, the drawdown at each well appears to follow the Theis curve, but at later times the drawdown falls below the Theis curve, indicating that the constant-potential boundary is affecting the data. Type curve analyses were performed on both wells, and transmissivities ($kh/\mu$) of $1.11 \times 10^6$ md·ft/cp and $1.76 \times 10^6$ md·ft/cp were obtained. Because fluid viscosity changes by a factor of 2.5 in the temperature range considered, the highly nonisothermal temperature distribution and proximity to the hot fault obscure the normal pressure-transient response. The effect of viscosity contrasts in nonisothermal well-test analysis has been discussed in Mangold et al. (1981). The present exercise seems to indicate that interference data may not be suitable for analysis by standard methods. However, if sufficiently accurate early-time production data are available, a value for the reservoir transmissivity may be obtained and the nature of the fault may be determined. This type of pressure-transient phenomena has been observed at the Susanville anomaly, where analysis of production data has given a transmissivity value of $7.3 \times 10^5$ md·ft/cp and where several observation wells have yielded transmissivities ranging from $2.3 \times 10^6$ to $3.6 \times 10^6$ md·ft/cp.

## PRODUCTION AND REINJECTION WELL SITING

Locating the production well as close as possible to the fault will allow production of the hottest fluid and will optimize the stimulation of recharge from a fault. Proper reinjection well siting is critical in fault-charged systems because an inappropriately placed reinjection well can create premature cooling of the production well. The criteria for reinjection well siting are as follows:

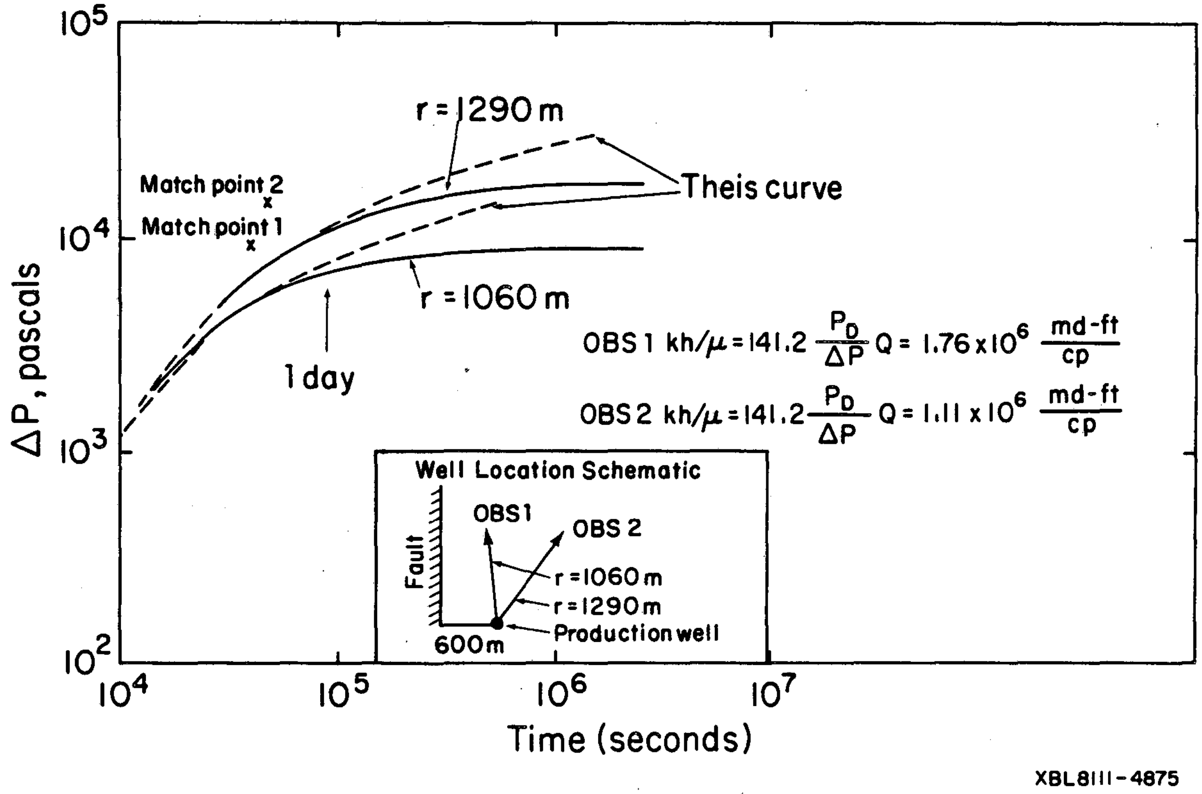


Figure 13. Drawdown and type curve analysis for the interference wells in an aquifer bounded by a constant-potential fault.

1. Reinjection should be done downstream from the production well.

2. If a constant-potential fault is present, care should be taken to locate the reinjection well so that the pressure buildup due to reinjection does not negate the production-enhanced flow from the fault. If the aquifer is sufficiently permeable (pressure support not needed) and if the produced fluids can be disposed of by some means other than reinjection, it may be desirable either not to reinject at all or to reinject far from both the production well and the fault.

3. The steady-state interflow between the production and injection wells should be minimized. With proper siting, interflow between the wells may be negligible in an aquifer with regional flow (DaCosta and Bennett, 1960).

## CONCLUSION

By using a newly developed computational model for fault-charged reservoirs and a numerical simulator (PT), the effects of hot water recharge into a near-surface hydrothermal aquifer have been included in reservoir engineering calculations. Key system parameters have been identified, the most important being the hydrologic characteristics of the fault itself. More simply, the ability of the fault to continue to provide hot water under production-induced reservoir conditions is critical to the longevity of the system. Two different boundary conditions for the fault have been investigated: constant-potential and constant-flow boundaries. The constant-flow case can be considered as a conservative one and the constant-potential case as optimistic.

The methodology discussed in this paper has been applied to the Susanville, California, hydrothermal resource. Predictions have been made of how the temperature will change with time, given a simple exploitation strategy.

Lifetime estimates and reservoir assessment using the methodology discussed herein are considerably more optimistic than those made if the hot water recharge into the system is ignored.

## ACKNOWLEDGEMENTS

This work was supported by the Assistant Secretary for Conservation and Renewable Energy, Office of Renewable Technology, Division of Geothermal and Hydropower Technologies of the U.S. Department of Energy under Contract No. DE-AC03-76SF00098.

NOMENCLATURE

$a$ = Geothermal gradient (°C/m)

$b$ = Aquifer thickness (m)

$c$ = Heat capacity (J/kg·°C)

$D$ = Thickness of caprock (m)

$H$ = Thickness of bedrock (m)

$k$ = Permeability (md, $10^{-15}$ $m^2$)

$\lambda$ = Thermal conductivity (J/m·s·°C)

$\mu$ = Viscosity (cp, $10^{-3}$ Pa·s)

$p$ = Laplace parameter

$\phi$ = Porosity

$q$ = Fault recharge rate ($m^3$/s·m)

$\rho c$ = Volumetric heat capacity (J/$m^3$·°C)

$t$ = Time (s)

$T$ = Temperature (°C)

$T_{b1}$ = Temperature at ground surface (°C)

$T_{b2}$ = Temperature of the bottom of the section (°C)

$u$ = Temperature in aquifer in Laplace domain

$v$ = Temperature in rock matrix above aquifer in Laplace domain

$w$ = Temperature in rock matrix below aquifer in Laplace domain

$x$ = Distance from the fault (m)

$z$ = Vertical coordinate (m)

Subscripts

$a$ = Aquifer

$f$ = Fault

$w$ = Liquid water

$r$ = rock matrix

REFERENCES

Benson, S.M., Goranson, C.B., Noble, J., Schroeder, R.C., Corrigan, D., and Wollenberg, H. (1980). Evaluation of the Susanville, California Geothermal Resource. Lawrence Berkeley Laboratory Report LBL-11187.

Bodvarsson, G.S. (1982). Mathematical Modeling of the Behavior of Geothermal Systems Under Exploitation (Ph.D. dissertation). Lawrence Berkeley Laboratory Report LBL-13937.

Bodvarsson, G.S., Miller, C.W., and Benson, S.M. (1981). A Simple Model for Fault-Charged Hydrothermal Systems Lawrence Berkeley Laboratory Report LBL-12869. (Also presented at the Geothermal Resources Council Annual Meeting, 1981, Houston, Texas.)

DaCosta, J.A., and Bennett, R.R. (1960). The Pattern of Flow in the Vicinity of a Recharging and Discharging Pair of Wells in an Aquifer Having Areal Parallel Flow. International Association of Scientific Hydrology, Publication 52, Commission of Subterranean Waters, p. 524-536.

Mangold, D.C., Tsang, C.F., Lippmann, M.J., and Witherspoon, P.A. (1981). A Study of Thermal Discontinuity in Well Test Analysis. Journal of Petroleum Technology, v. 33, no. 6 (June).

*TECHNICAL INFORMATION DEPARTMENT*
*LAWRENCE BERKELEY LABORATORY*
*UNIVERSITY OF CALIFORNIA*
*BERKELEY, CALIFORNIA 94720*